Biogeosciences

Air-sea CO$_2$ fluxes on the Bering Sea shelf

N. R. Bates[1]**, J. T. Mathis**[2]**, and M. A. Jeffries**[3]

[1]Bermuda Institute of Ocean Sciences, Ferry Reach, Bermuda
[2]University of Alaska-Fairbanks, Fairbanks, USA
[3]University of Victoria, Victoria, Canada

Abstract. There have been few previous studies of surface seawater CO$_2$ partial pressure (pCO$_2$) variability and air-sea CO$_2$ gas exchange rates for the Bering Sea shelf. In 2008, spring and summertime observations were collected in the Bering Sea shelf as part of the Bering Sea Ecological Study (BEST). Our results indicate that the Bering Sea shelf was close to neutral in terms of CO$_2$ sink-source status in springtime due to relatively small air-sea CO$_2$ gradients (i.e., ΔpCO$_2$) and sea-ice cover. However, by summertime, very low seawater pCO$_2$ values were observed and much of the Bering Sea shelf became strongly undersaturated with respect to atmospheric CO$_2$ concentrations. Thus the Bering Sea shelf transitions seasonally from mostly neutral conditions to a strong oceanic sink for atmospheric CO$_2$ particularly in the "*green belt*" region of the Bering Sea where there are high rates of phytoplankton primary production (PP)and net community production (NCP). Ocean biological processes dominate the seasonal drawdown of seawater pCO$_2$ for large areas of the Bering Sea shelf, with the effect partly countered by seasonal warming. In small areas of the Bering Sea shelf south of the Pribilof Islands and in the SE Bering Sea, seasonal warming is the dominant influence on seawater pCO$_2$, shifting localized areas of the shelf from minor/neutral CO$_2$ sink status to neutral/minor CO$_2$ source status, in contrast to much of the Bering Sea shelf. Overall, we compute that the Bering Sea shelf CO$_2$ sink in 2008 was 157 ± 35 Tg C yr^{-1} (Tg = 10^{12} g C) and thus a strong sink for CO$_2$.

1 Introduction

The Bering Sea shelf is one of the most productive marine ecosystems in the global ocean. Physical processes and seasonal sea-ice advance and retreat in the Bering Sea play a major role in controlling water mass properties and shaping the character of pelagic and benthic ecosystems found on the shelf. On the extensive continental shelf (Fig. 1), seasonally high rates of pelagic phytoplankton primary production (PP) supports large populations of marine mammals and seabirds, and coastal fisheries of Alaska. On the outer shelf of the Bering Sea, a region of elevated phytoplankton biomass termed the "*green belt*" has been observed in spring and summer for many decades (Hansell et al., 1989; Springer et al., 1996; Okkonen et al., 2004; Mathis et al., 2010). Extensive, but sporadic blooms of coccolithophores, which are CaCO$_3$-producing phytoplankton (class Prymnesiophyceae) have also been observed in the SE Bering Sea shelf (e.g., Stockwell et al., 2001; Broerse et al., 2003; Merico et al., 2004, 2006). In contrast to the shelf, the open ocean regions of the western Bering Sea is much less productive and has been described as a high nutrient, low chlorophyll (HNLC) region (Banse and English, 1999).

Over the last few decades, many studies have been conducted on the physical and biological character of the Bering Sea, but there have been few studies of the marine carbon cycle, air-sea CO$_2$ exchange rates or the potential impact of ocean acidification on the chemistry of shelf waters and ecosystems of the Bering Sea. In the open-ocean region of the Bering Sea, observations of seawater pCO$_2$ (i.e., partial pressure of CO$_2$) and dissolved inorganic carbon (DIC) have been collected close to the western Aleutian Islands (e.g., Murphy et al., 2001; Nedashkovkii and Sapozhnikov, 2001; Wong et al., 2002; Murata and Takazawa, 2002) or outside the Bering Sea in the subarctic gyre of the North Pacific

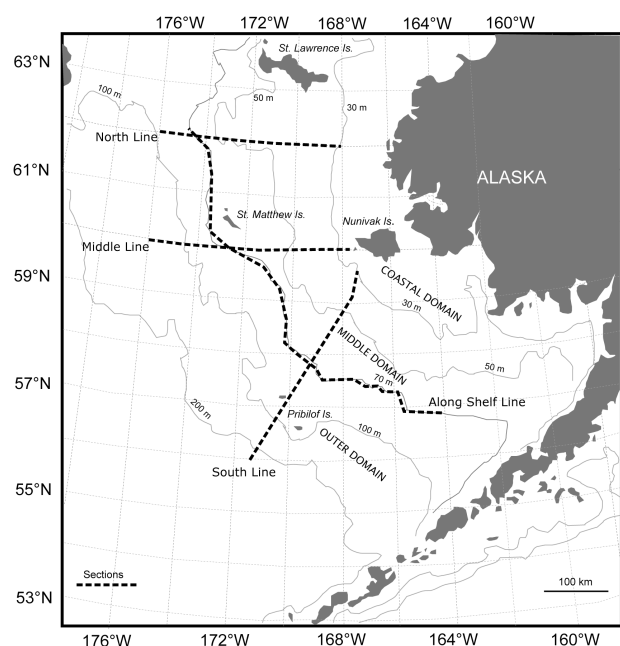*Correspondence to:* N. R. Bates
(nick.bates@bios.edu)

Fig. 1. Bering Sea shelf location map. The approximate positions of the North Line, Middle Line, South Line, and Along Shelf Line transects are shown on the figure. Approximate locations of the Coastal, Middle and Outer domains of the shelf are also shown.

Ocean (e.g., Midorikawa et al., 2002). On the Bering Sea shelf, a few studies have shown that high summertime levels of phytoplankton primary production observed in the "*green belt*" result in a drawdown of seawater inorganic nutrients and DIC (and pCO_2) (e.g., Kelley and Hood, 1971; Park et al., 1974; Codispoti et al., 1982, 1986; Chen and Gao, 2007; Mathis et al., 2010). Extensive coccolithophore blooms on the SE Bering Sea shelf should also seasonally decrease total alkalinity (TA) and DIC of seawater (as observed in other coastal seas and oceans; e.g., Robertson et al., 1994; Bates et al., 1996a), but at present, there has only been limited assessments of the impact of coccolithophores on the ocean carbon cycle of the Bering Sea (Murata and Takizawa, 2002, Murata, 2006; Merico et al., 2004, 2006). Unlike other taxonomic classes of phytoplankton blooms, coccolithophores can increase seawater pCO_2 content and thus contribute to a negative coccolithophore-CO_2 feedback (Riebesall et al., 2000; Zondervan et al., 2001; Ridgwell et al., 2007) that has potentially important implications for the role of the global ocean in the uptake of anthropogenic CO_2, modulation of atmospheric CO_2 and climate responses over the next few centuries.

The contribution of the Bering Sea to the global ocean uptake of CO_2 is also highly uncertain. Early studies based on observations (Codispoti et al., 1982, 1986) and models (Walsh and Dieterle, 1994; Walsh et al., 1996) suggested that the entire Bering Sea was a potential sink for atmospheric CO_2. More recently, it has been reported that the

Bering Sea acts as a net annual oceanic sink of CO_2 on the order of 200 Tg C yr^{-1} (Tg = 10^{12} g C; Chen et al., 2004) and thus a significant contributor (>10 %) to the annual global uptake of CO_2 ($\sim$1.4 Pg yr^{-1}; Takahashi et al., 2009). However, the seawater pCO_2 datasets of Takahashi et al. (2002, 2009) suggest that the open-ocean Bering Sea exhibits seasonal changes from a CO_2 sink in springtime (due to phytoplankton primary production) to a CO_2 source to the atmosphere in summertime (Takahashi et al., 2002). But, important caveats to note are that the seawater pCO_2 climatology has a coarse spatial resolution of $4° \times 5°$ and data was primarily collected from a relatively small open-ocean region of the Bering Sea (just north of the Aleutian Islands). Indeed, in the recent Takahashi et al. (2009) seawater pCO_2 climatology, only one cruise dataset across the Bering Sea shelf was deemed of sufficient quality to be included in the climatology.

Given the above uncertainties about the contribution of the Bering Sea shelf to the global ocean uptake of CO_2, it is important to improve assessments of the rate of air-sea CO_2 exchange for this coastal sea. In this paper, we examine the seasonal variability of inorganic carbon for the Bering Sea shelf observed in 2008 and determine the magnitude and timing of ocean CO_2 sinks and sources. We compare our observations with average conditions using the seawater pCO_2 climatology of Takahashi et al. (2009) and a seawater pCO_2 climatology based on a multiple-linear regression (MLR) model. Such assessment also serve as a baseline for understanding the potential changes in ocean CO_2 sinks and sources in responses to changes in physical forcing (e.g., circulation and mixing; nutrient supply; sea-ice advance/retreat timing and sea-ice extent; summer heating/winter cooling) and marine ecosystems (e.g., the rate, extent, timing and community structure of the spring phytoplankton bloom; presence/absence of coccolithophores, Stockwell et al., 2001). In companion papers, the rate of net community production (NCP; Mathis et al., 2010) and the impact of ocean acidification on the seawater carbonate chemistry of the Bering Sea shelf (Mathis et al., 2011) have been reported.

2 Methods and materials

2.1 Physical and biological setting of the Bering Sea

The subpolar Bering Sea is a semi-enclosed basin (Fig. 1) with an extensive continental shelf in the east and deep open-ocean to the west. Physical processes and seasonal sea ice cover in the Bering Sea play a major role in controlling water mass properties and shaping the character of shelf pelagic and benthic ecosystems (e.g., McRoy and Goering, 1974; Wyllie-Echeverria and Ohtani, 1999; Stabeno et al., 2002; Grebmeier et al., 2006a, b). During the winter, sea-ice covers much of the Bering Sea shelf, but the advance is constrained by the presence of relatively warm water in the central and

southern Bering Sea. During winter, water-masses are confined to a small range of temperature-salinity through vertical homogenization by ventilation, brine rejection and mixing. During the summertime, sea-ice retreats into the Chukchi Sea and Canada Basin of the Arctic Ocean. The extent of sea-ice cover and ecosystem structure undergoes significant interannual changes (e.g., Stabeno et al., 2001; Macklin et al., 2002; Hunt et al., 2002) that appear related to climatological changes in the Pacific Decadal Oscillation (PDO), Arctic Oscillation (AO) and El Niño-Southern Oscillation (ENSO), as well as long-term reduction in sea-ice extent (e.g., Springer, 1998; Hollowed et al., 2001; Hunt et al., 2002; Rho and Whitledge, 2007) that is linked to amplification of warming in the Arctic and sub-Arctic with subsequent reductions in sea-ice extent and thickness (e.g., Serreze et al., 2007).

An extensive (>1000 km length) and broad (>500 km width) shelf, winter-time cross-shelf renewal of nutrients, vertical stability imposed by the flux of river runoff from the continent as well as by sea-ice formation and melt, and long hours of irradiance throughout the spring and summer, makes the Bering Sea shelf one of the most productive marine ecosystems in the world (e.g., Springer et al., 1996; Grebmeier et al., 2006a, b; Rho and Whitledge, 2007). Over the past decade, the character of the marine ecosystem in the Bering Sea has exhibited considerable change (e.g., Stabeno et al., 2001; Macklin et al., 2002; Hunt et al., 2002; Bond et al., 2003; Bond and Overland, 2005; Grebmeier et al., 2006b; 2008). Cold-water, Arctic species have been replaced by organisms more indicative of temperate zones and reduced sea-ice cover has been proposed to favor a 'phytoplankton–zooplankton' dominated ecosystem over the more typical "sea-ice algae–benthos" ecosystem indicative of Arctic Ocean shelves (including the northern Bering Sea shelf) in particular (Piepenburg, 2005). Large, sweeping populations of jellyfish have come and gone (Napp et al., 2002), and coccolithophorid blooms that had become regular features of the SE Bering Sea (e.g., Stockwell et al., 2001; Broerse et al., 2003; Merico et al., 2004, 2006) have also been absent over the last few years. Further changes in physical forcings to the Bering Sea (Stabeno et al., 2001) will likely lead to further dynamic changes in the marine ecosystem, with uncertain feedbacks to the marine carbon cycle.

2.2 Marine carbon cycle measurements and considerations

Physical and biogeochemical measurements (including marine carbon cycle observations) were collected in the Bering Sea shelf from the US Coast Guard Cutter Healy during two cruises in 2008 as part of the Bering Sea Ecological Study (BEST) program (http://www.eol.ucar.edu/projects/best/). During spring (27 March–6 May; HLY 08-02) and summer (July 3–31; HLY 08–03) cruises, 67 and 84 CTD-hydrocast stations were occupied across the Bering Sea shelf on three east to west transects (North Line, Middle

Line and South Line) and one north-south transect (Fig. 1; Mathis et al., 2010). These transects sampled the shallow Coastal (<50 m deep); Middle (∼50–100 m deep) and Outer (>100 m deep) domains of the Bering Sea shelf (Fig. 1). At each hydrocast station, conductivity-temperature-depth (CTD) profiles were collected using Seabird SBE-911 sensors while seawater samples were collected from Niskin samplers at representative depths for a suite of biogeochemical measurements (i.e., dissolved oxygen, inorganic nutrients). Shipboard sea-ice observations were retrieved from field reports (http://www.eol.ucar.edu/projects/best/). Sea-ice cover was typically in the range of 90–100 % at most stations (with the exception of minor flaw leads; and south of the Pribilof Islands and SE Bering Sea) during the spring cruise while the summer cruise was sea-ice free.

Samples for seawater carbonate chemistry were taken at most CTD/hydrocast stations on both spring and summer cruises. DIC and TA samples were drawn from Niskin samplers into clean $0.3 \, dm^3$ size Pyrex glass reagent bottles, using established gas sampling protocols (Bates et al., 1996a; Dickson et al., 2007). A headspace of <1 % of the bottle volume was left to allow for water expansion and all samples were poisoned with 200 µl of saturated $HgCl_2$ solution to prevent biological alteration, sealed and returned to UAF for analysis. DIC was measured by a gas extraction/coulometric technique (see Bates et al., 1996a, b for details), using a VINDTA 3C instrument (Marianda Co.) that controls the pipetting and extraction of seawater samples and a UIC CO_2 coulometer detector. The precision of DIC analyses of this system was typically better than 0.05 % (∼1 µmoles kg^{-1}). TA was determined by potentiometric titration with HCl (see Bates et al., 1996a, b for details) using the VINDTA system. Seawater certified reference materials (CRM's; prepared by A. G. Dickson, Scripps Institution of Oceanography; http//www.andrew.ucsd.edu) were analyzed to ensure that the accuracy of DIC and TA was within 0.1 % (∼2 µmoles kg^{-1}).

The complete seawater carbonic acid system (i.e., CO_2, H_2CO_3, HCO_3^-, CO_3^{2-}, H^+) can be calculated from two of five measureable carbonate system parameters (i.e., DIC, TA, pCO_2, pH, and more recently CO_3^{2-}), along with temperature and salinity (Zeebe and Wolf-Gladrow, 2001; Dickson et al., 2007). The carbonic acid dissociation constants (pK_1 and pK_2) of Mehrbach et al. (1973), as refit by Dickson and Millero (1997), were used to calculate seawater pCO_2 and other carbonate parameters, using the equations of Zeebe and Wolf-Gladrow (2001). In addition, the CO_2 solubility equations of Weiss (1974), and dissociation constants for borate (Dickson, 1990), and phosphate (Dickson et al., 2007) were used. The calculation of seawater pCO_2 has an error of ∼5–10 µatm depending on pK_1 and pK_2 used (i.e., Mehrbach et al., 1973, as refit by Dickson and Millero, 1997; Goyet and Poisson, 1989; Roy et al., 1993; Millero et al., 2006). These calculations were cross-checked with the CO2calc program (Robbins et al., 2010). The difference in calculated seawater
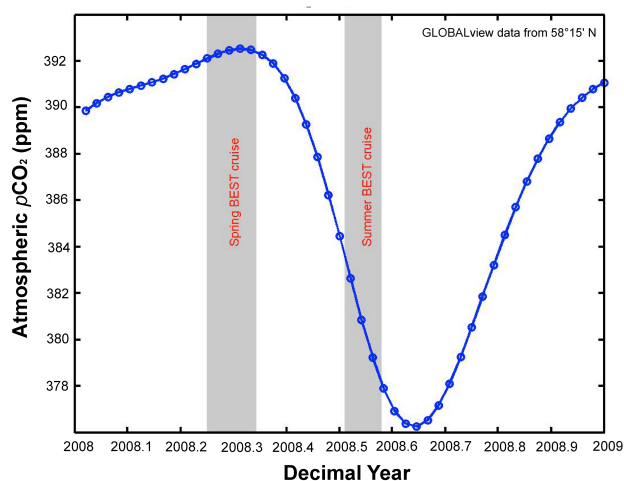
Fig. 2. Atmospheric CO$_2$ values (ppm) for the Bering Sea from GLOBALVIEW for 2008 (http://www.esrl.noaa.gov/gmd/ccgg/globalview/). The shaded areas represent the periods of time that the cruises were taking place. Atmospheric CO$_2$ values were then interpolated to the time each CTD hydrocast was conducted.

Fig. 3. Surface windspeed observations (m s^{-1}) from the USCGC *Healy* for both the spring (top plot) and summer (bottom plot) 2008 BEST cruises. In each plot, the original hourly wind data is shown in blue (spring) and red (summer) with the 6-hour running mean shown in green. The grey lines indicate times of CTD casts.

pCO$_2$ using different pK$_1$ and pK$_2$ was relatively small ($<5\,\mu$atm) at temperatures less than 0 °C (Bates, 2006), increasing to $\sim$10–15 µatm in warmer waters (8–12 °C). Overall, the mean difference in calculated seawater pCO$_2$ was small ($<10\,\mu$atm) compared to the large range of seawater pCO$_2$ values ($>200\,\mu$tm) observed across the Bering Sea shelf.

2.3   Calculation of air-sea CO$_2$ gas exchange rates

The net air-sea CO$_2$ flux (F) was determined by the following formula:

$$F = ks(\Delta p\mathrm{CO}_2) \qquad (1)$$

where k is the transfer velocity, s is the solubility of CO$_2$ and, ΔpCO$_2$ is the difference between atmospheric and oceanic partial pressures of CO$_2$. The ΔpCO$_2$, or air-sea CO$_2$ disequilibrium, sets the direction of CO$_2$ gas exchange while k determines the rate of air-sea CO$_2$ transfer. Here, gas transfer velocity-wind speed relationships for long-term wind conditions based on a quadratic (U^2) dependency between wind speed and k (i.e., Wanninkhof, 1992) were used to determine air-sea CO$_2$ fluxes:

$$k = 0.39\, U_{10}^2\, (Sc/660)^{-0.5} \qquad (2)$$

where U_{10} is wind speed corrected to 10 m, and Sc is the Schmidt number for CO$_2$. The Schmidt number was calculated using the equations of Wanninkhof (1992) and s (solubility of CO$_2$ per unit volume of seawater) was calculated from the observed temperature and salinity using the equations of Weiss (1974). Estimates of net air-sea CO$_2$ flux rates
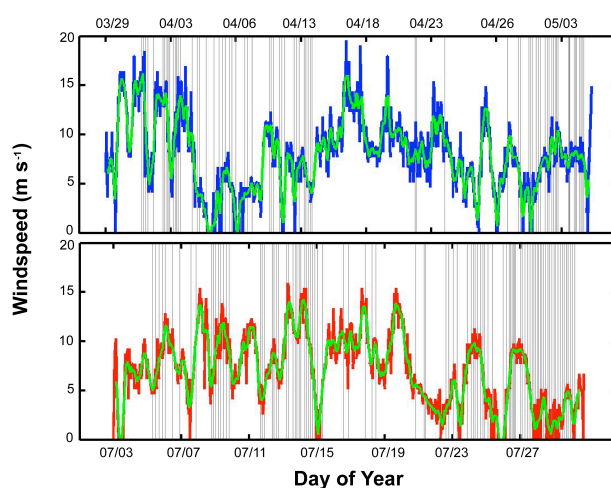
for the Bering Sea shelf were made using two methods: (1) calculating net air-sea CO$_2$ flux rates at each hydrocast station using seawater pCO$_2$ and ΔpCO$_2$ data, and: (2) using interpolation and extrapolation techniques, and a multiple linear regression (MLR) method to produce modelled maps of seawater pCO$_2$ and ΔpCO$_2$ from which air-sea CO$_2$ flux rates were computed across the Bering Sea with a spatial resolution of 1° and temporal resolution of 1 month (Sect. 2.4).

Net air-sea CO$_2$ flux rates were computed at each hydrocast station using surface seawater observations and atmospheric pCO$_2$ data to compute ΔpCO$_2$ values. Atmospheric pCO$_2$ data were determined using monthly-resolved latitudinal marine boundary layer atmospheric CO$_2$ distribution extrapolated to all longitudes. These values were obtained from GLOBALVIEW (http://www.esrl.noaa.gov/gmd/ccgg/globalview/; GLOBALVIEW-CO$_2$, 2007; Fig. 2), and corrected for water vapor pressure. Although synoptic meteorological data (including windspeed) was collected from the USCGC *Healy* during the cruises (Fig. 3), this data was not used to calculate air-sea CO$_2$ flux rates. Instead, ΔpCO$_2$ values and daily averaged 6-hourly wind speed data from the NCEP (National Centers for Environmental Prediction)/NCAR (National Center for Atmospheric Research) reanalysis 2 data assimilation model was used to calculate k values (http://www.cdc.noaa.gov/cdc/data.ncep.html) and net air-sea CO$_2$ flux rates. NCEP/NCAR Reanalysis 2 (i.e. NNR) data was used rather than shipboard meteorological data reports in order to allow estimates of air-sea CO$_2$ fluxes across the Bering Sea to be made. The spatial resolution of the NNR data assimilation model windspeed dataset is 2.5° by 2.5°. In regions where 1° × 1° ΔpCO$_2$ values
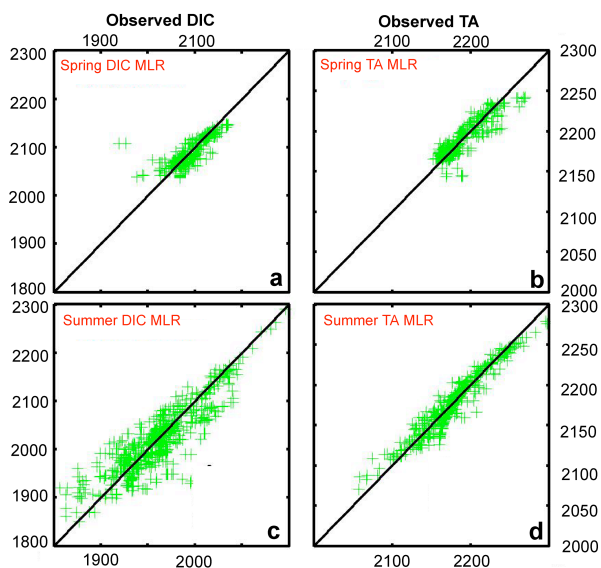
Fig. 4. (a) Interpolation of observed DIC using MLR approaches for the 2008 spring BEST cruise (std.dev 12.7 μmoles kg^{-1}; r^2 = 0.63; $n = 368$); **(b)** Interpolation of observed TA using MLR approaches for the 2008 spring BEST cruise (std.dev 8.4 μmoles kg^{-1}; $r^2 = 0.78$; $n = 368$); **(c)** Interpolation of observed DIC using MLR approaches for the 2008 summer BEST cruise (std.dev 27.9 μmoles kg^{-1}; $r^2 = 0.76$; $n = 582$); **(d)** Interpolation of observed TA using MLR approaches for the 2008 summer BEST cruise (std.dev 6.7 μmoles kg^{-1}; $r^2 = 0.92$; $n = 582$).

overlapped the 2.5° by 2.5° NNR data, the average NNR windspeed data was used.

2.4 MLR based model considerations

Inorganic carbon observations of the global ocean typically have limited temporal and spatial coverage compared to other hydrographic properties such as temperature, salinity, dissolved oxygen and inorganic nutrients. Due to data limitations, multiple linear regression (MLR) approaches have often been used to interpolate and extrapolate available inorganic carbon data to ocean basins and the global ocean (e.g., Goyet and Davis, 1997; Goyet et al., 2000; Lee, 2001; Lee et al., 2002; Bates et al., 2006a, b). Similar interpolation and extrapolation techniques have been used to yield global estimates of air-sea CO$_2$ exchange rates using available surface seawater pCO$_2$ observations (Takahashi et al., 2002; 2009). In this study, we compared our calculated seawater pCO$_2$ with the data-based seawater pCO$_2$ climatology of Takahashi et al. (2009) that has a spatial resolution of 4°× 5°. In addition, we also compared calculated seawater pCO$_2$ data with a MLR-based model, similar to other studies (e.g., Lee, 2001; Lee et al., 2002; Bates et al., 2006a, b), to produce a data-based seawater pCO$_2$ climatology map of the Bering Sea shelf with improved spatial resolution (i.e., 1°× 1°).

Using MLR methods, interpolation of DIC and TA distributions from other hydrographic properties such as temperature, salinity, and inorganic nutrients has an uncertainty of ∼5–15 μmoles kg^{-1} when applied to data below the mixed layer (e.g., Goyet and Davis, 1997; Sabine et al., 1999; Sabine and Feely, 2001; Coatanoan et al., 2001; Key et al., 2004). In the mixed layer, the interpolation of DIC and TA has larger uncertainty due to seasonal variability. Here, a MLR-based model is used to interpolate DIC and TA data from observed hydrographic properties using observed seawater carbonate chemistry data collected in the Bering Sea shelf in 2008. Interpolated data were then extrapolated to the entire Bering Sea shelf using climatological hydrographic data from the World Ocean Atlas (WOA, 2005) that has a spatial resolution of 1°× 1°, vertically differentiated into 14 layers in the upper 500 m with a temporal resolution of 1 month. Climatological surface seawater pCO$_2$ maps for the Bering Sea shelf were then calculated from these DIC and TA fields (using the same approach outlined in Sects. 2.2 and 2.3). The seasonal and annual rates of air-sea CO$_2$ exchange were then compared with data-based seawater pCO$_2$ climatology maps (Takahashi et al., 2002, 2009). Given that our data collection during 2008 was shelf-based, we do not report seawater carbonate chemistry extrapolated to the western open-ocean Bering Sea.

2.4.1 Interpolation and extrapolation techniques

Several interpolation schemes were investigated using the Bering Sea shelf DIC and TA data including variables such as: temperature (T), salinity (S), oxygen anomaly (O$_2$a), nitrate (NO$_3$), phosphate (PO$_4$), silicate (SiO$_4$), depth (z), latitude and longitude. The oxygen anomaly was defined as the dissolved oxygen minus the oxygen saturation where the saturation level was calculated from the bottle temperature and salinity data. Different combinations of parameters were tested in order to improve the quality of fit and to reduce the residual errors between the synthetic and measured data. The optimal fit was determined by examining the RMS error, the comparison of the synthetic versus measured data and the spatial pattern of the residuals. We found that the optimal interpolation with the lowest associated uncertainties for DIC and TA (generally for the 0–500 m depth) were a function of the following properties:

$$\text{DIC} = \alpha_1 + \alpha_2 T \alpha_3 S + \alpha_4 z + \alpha_5 \text{lat} + \alpha_6 \text{NO}_3 + \alpha_7 \text{O}_2 a + \alpha_8 \text{SiO}_4 \quad (3)$$

$$\text{TA} = \beta_1 + \beta_2 T \beta_3 S + \beta_4 z + \beta_5 \text{lat} + \beta_6 \text{NO}_3 + \beta_7 \text{O}_2 a + \beta_8 \text{SiO}_4 \quad (4)$$

where α and β are the regression coefficients for DIC and TA, respectively. Inclusion of PO$_4$ or longitude did not improve the regressions. For 2008 spring BEST data, the best-fit MLR regression had an uncertainty of ∼12.7 and 8.4 μmoles kg^{-1}, for DIC and TA, respectively (Fig. 4). For summer data, the best-fit MLR regression had an uncertainty of ∼27.9 and 6.7 μmoles kg^{-1} for DIC and TA, respectively (Fig. 4).
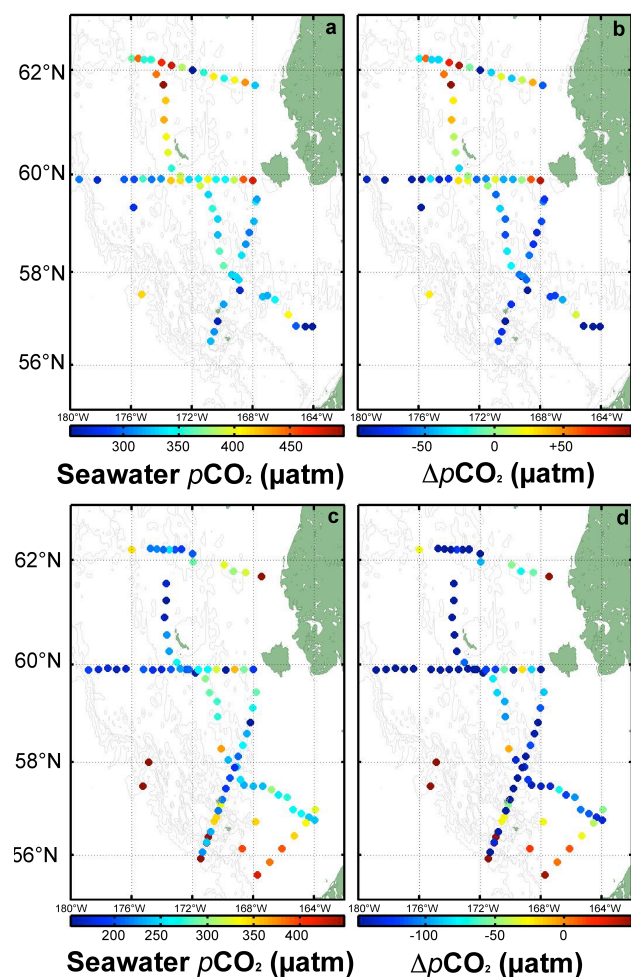
Fig. 5. Surface seawater pCO_2 (calculated from DIC and TA) and ΔpCO_2 values observed at hydrocast stations in spring and summertime during the 2008 BEST program. **(a)** Calculated surface seawater pCO_2 during the 2008 spring BEST cruise; **(b)** Calculated seawater ΔpCO_2 station during the 2008 spring BEST cruise; **(c)** Calculated seawater pCO_2 during the 2008 summer BEST cruise; **(d)** Calculated seawater ΔpCO_2 during the 2008 summer BEST cruise.

Fig. 6. Surface climatological maps of seawater carbonate properties and air-sea CO_2 flux determined using the MLR-based model. **(a)** springtime DIC (μmoles kg^{-1}); **(b)** summertime DIC (μmoles kg^{-1}); **(c)** springtime seawater pCO_2 (μatm); **(d)** summer seawater pCO_2 (μatm); **(e)** springtime air-sea CO_2 flux (mmoles m^{-2} d^{-1}); **(f)** summertime air-sea CO_2 flux (mmoles m^{-2} d^{-1}).

MLR regression coefficients were then applied to the World Ocean Atlas 2005 (WOA2005) data for temperature (Locarnini et al., 2006), salinity (Antonov et al., 2006), oxygen (Garcia et al., 2006a) and inorganic nutrient (Garcia et al., 2006b) climatology datasets. This provides extrapolated MLR based maps of mean DIC and TA for the Bering Sea shelf that had a spatial resolution of $1° \times 1°$ and temporal resolution of 1 month. The modelled MLR data has a vertical resolution of 14 layers in the upper 500 m and typically 4–10 layers ($\sim$30–200 m) for the Bering Sea shelf. Surface seawater pCO_2 fields for the Bering Sea were then calculated from MLR based model DIC and TA maps (using the same approach outlined in Sects. 2.2 and 2.3). An impor-
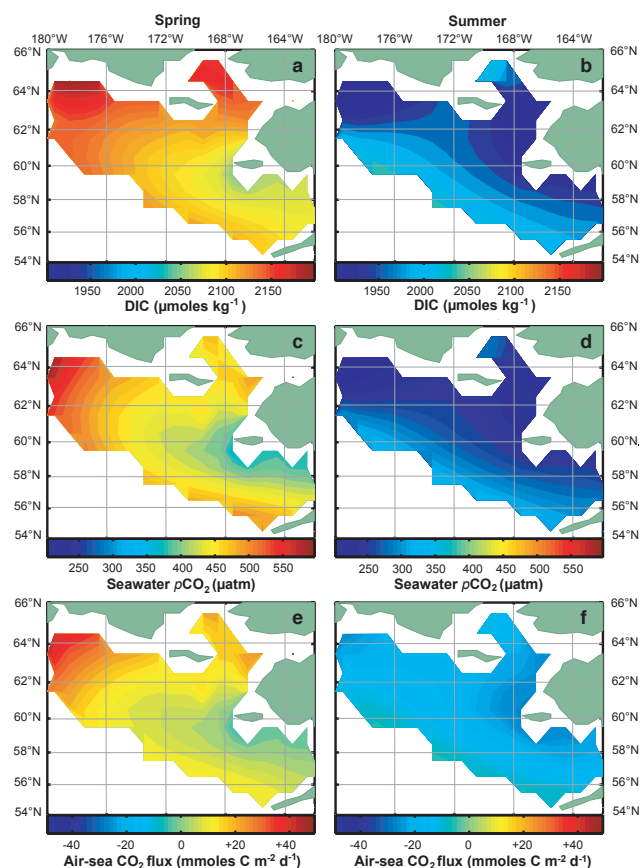
tant consideration is that modeled MLR maps of DIC, TA and pCO_2 provide a climatological view of seawater carbonate chemistry conditions in the Bering Sea shelf rather than a model simulation of 2008 conditions. The MLR regression coefficients are based on observed DIC, TA and hydrographic data, but the MLR model extrapolation uses climatological, mean values of temperature, salinity, dissolved oygen and inorganic nutrients from the World Ocean Atlas (WOA2005) to compute climatologically based DIC and TA maps.

Errors in the MLR analysis arise from a combination of interpolation and extrapolation errors. Interpolation errors stemmed from the goodness-of-fit of the empirical linear function, where one standard deviation was used to quantify the error. Extrapolation errors arose from applying the regression coefficients to areas of the Bering Sea that have inadequate spatial coverage of data (i.e., open-ocean).

Net air-sea CO_2 flux rates were also computed using surface seawater pCO_2 and ΔpCO_2 maps derived from MLR

interpolation and extrapolation. Marine boundary layer atmospheric CO_2 distribution extrapolated to all longitudes were obtained from GLOBALVIEW (GLOBALVIEW-CO_2, 2007). Daily averaged 6-hourly NNR wind speed data was used to calculate k values.

As mentioned earlier, there are many sources of error in an analysis such as this and how they are propagated through the analysis determines how large the error will be on the final air-sea CO_2 flux estimates. Quantifying the error of the interpolation comes directly from the regression models (RMS) where a Monte Carlo method was used to propagate the error from the DIC and TA fields creating a reliable error estimate for the seawater pCO_2 field. For each point, we calculated the pCO_2 a thousand times while randomizing the error at each DIC and TA node. Using an analysis such as this, the mean of the simulation should converge on the estimated pCO_2 field with a reliable error estimate without having to use a brute force method that would maximize the error. Because there was an error estimate for every estimated DIC and TA point from the MLR analysis, there is an associated unique pCO_2 error for every point as well. It was found that the average seawater pCO_2 error for the Bering Sea shelf was 15.2 µatm, relatively small compared to seasonal changes of seawater pCO_2.

3 Results

3.1 Seawater pCO_2 and ΔpCO_2 variability on the Bering Sea shelf

3.1.1 Spring observations of seawater pCO_2 and ΔpCO_2

Spring observations of surface (upper 10 m) seawater pCO_2 ranged from $\sim$180 µatm to $\sim$520 µatm across the Bering Sea shelf. ΔpCO_2 values ranged from ~ -200 µatm to $\sim$+130 µatm (Fig. 5) with large spatial variability in the potential for uptake of atmospheric CO_2 or release of CO_2 from the ocean to the atmosphere. In those regions where the potential to uptake atmospheric CO_2 existed, the SE Bering Sea shelf exhibit the strongest air-sea CO_2 gradients with surface seawater pCO_2 values very low ($\sim$180–200 µatm) and ΔpCO_2 values highly negative (~ -200–180 µatm). Elsewhere across the Bering Sea shelf, particularly between Nunivak Island and the Pribilof Islands, and the outer shelf west of St. Matthew Island, seawater pCO_2 values typically ranged from $\sim$260–330 µatm and ΔpCO_2 values were negative (~ -130 to -55 µatm). For comparison, Chen (1993) observed wintertime ΔpCO_2 values of ~ -50 to -70 µatm in the region west of St. Matthew Island ($\sim$58° N–62° N/171° W to 179° W) in 1983. In most other regions, seawater pCO_2 values from the spring 2008 BEST cruise were similar to atmospheric pCO_2 values. In the northern Bering Sea shelf, seawater pCO_2 values ranged

from $\sim$340–520 µatm. ΔpCO_2 values were positive close to Nunivak Island ($\sim$+60–80 µatm), just west of St. Matthew Island (up to +130 µatm), at the outermost shelf stations of the northern line (up to +90 µatm), and at a few deep (offshelf) Bering Sea stations. As such, these surface waters had the potential to release CO_2 to the atmosphere.

In comparison to the observations, the MLR based model maps of surface seawater pCO_2 indicate that Bering Sea shelf waters typically ranged from $\sim$350–450 µatm (ΔpCO_2 values of ~ -50 to +50 µatm) increasing from the inner shelf to the outer shelf and deep Bering Sea (Fig. 6). There were large differences evident between the 2008 spring (and summer) observations and the MLR based model maps. An explanation for the difference is that the MLR model maps, which are based on mean hydrographic values reported in the WOA2005 climatology rather than actual observed hydrography in the Bering Sea in 2008, simulate a "mean" state or climatology for seawater pCO_2 rather than a simulation of 2008 conditions driven by actual hydrography. Thus, calculated pCO_2 values were much lower in 2008 for springtime compared to MLR based Bering Sea shelf seawater pCO_2 that is based on a hydrographic climatology.

3.1.2 Summer observations of seawater pCO_2 and ΔpCO_2

Summertime observations of surface seawater pCO_2 exhibited a greater range ($\sim$130 µatm to $\sim$640 µatm) than springtime with most of the Bering Sea shelf strongly undersaturated with respect to the atmosphere (Fig. 5). The lowest surface seawater pCO_2 values were observed in the "*green belt*" of the middle and outer shelf between the northern and southern Bering Sea shelf (between Nunivak Island and the Pribilof Islands). In this regions, ΔpCO_2 values ranged from ~ -250 to -50 µatm and surface waters had a very strong potential to uptake atmospheric CO_2. In these areas, rates of NCP ranged from $\sim$22–35 mmoles C m^{-2} d^{-1} (Mathis et al., 2010). In the SE Bering Sea, in contrast to the "*green belt*" of the shelf, surface seawater pCO_2 had increased from springtime values of $\sim$180–200 µatm) µatm to $\sim$330–425 µatm reducing the driving force for uptake of atmospheric CO_2. At the innermost stations of the northern Bering Sea shelf and just south of the Pribilof Islands, surface seawater pCO_2 had high values (up to $\sim$670 µatm). Thus in contrast with much of the shelf, these relatively small areas had a strong potential to release CO_2.

In comparison to the observations, the MLR based maps indicate that summertime Bering Sea shelf waters typically ranged from $\sim$200–300 µatm (ΔpCO_2 values of ~ -150 to -100 µatm), increasing from the inner shelf to the outer shelf and deep Bering Sea (Fig. 6), and also in the SE Bering Sea shelf region. Calculated pCO_2 values were much lower in 2008 in summertime compared to the MLR based Bering Sea seawater pCO_2 climatology.
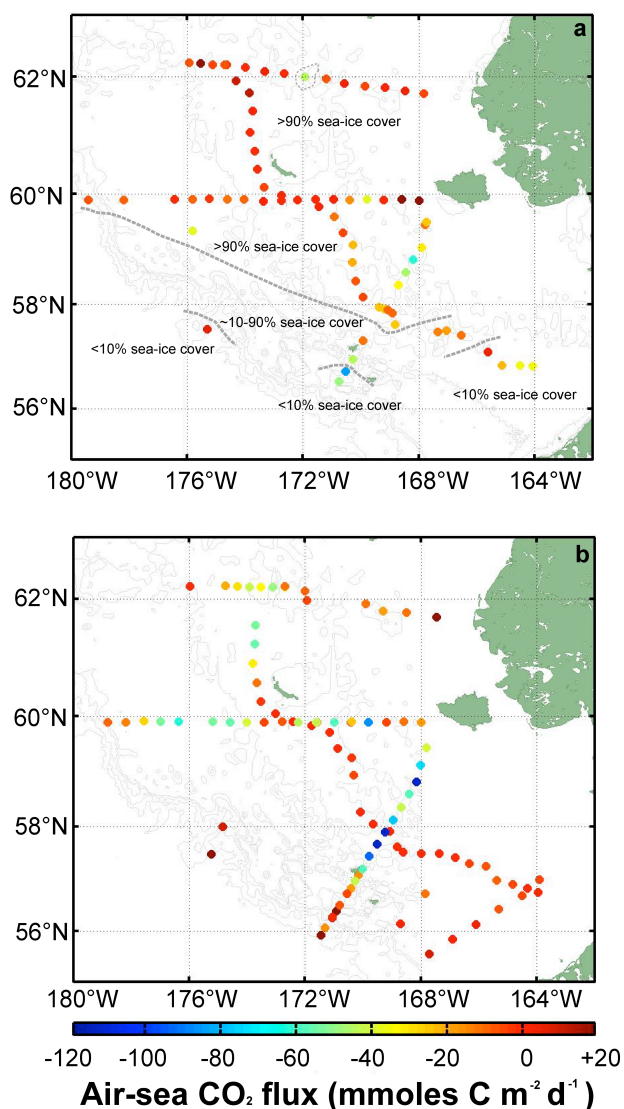
Fig. 7. Air-sea CO$_2$ flux values calculated at each CTD/hydrocast station in spring and summertime during the 2008 BEST program. **(a)** Estimated air-sea CO$_2$ flux (mmoles CO$_2$ m^{-2} d^{-1}) during the 2008 spring BEST cruise; **(b)** Estimated air-sea CO$_2$ flux (mmoles CO$_2$ m^{-2} d^{-1}) during the 2008 summer BEST cruise. Approximate sea-ice cover in shown in panel **(a)**. The influence of sea-ice as a barrier to gas exchange is discussed in Sect. 4.2.1

3.2 Air-sea CO$_2$ fluxes on the Bering Sea shelf

3.2.1 Springtime air-sea CO$_2$ fluxes

In springtime, potential air-sea CO$_2$ flux rates in the northern Bering Sea shelf varied between ∼0 and −10 mmoles CO$_2$ m^{-2} d^{-1} (negative values denote ocean CO$_2$ sink), with the outer stations exhibiting the potential for efflux of CO$_2$ up to ∼+25 mmoles CO$_2$ m^{-2} d^{-1} (Fig. 7). In the middle Bering Sea shelf, potential air-sea CO$_2$ flux rates were close

to neutral (between ∼0 and −10 mmoles CO$_2$ m^{-2} d^{-1}) particularly to the west of St. Matthew Island. There were localized areas of surface water that acted as potentially larger sinks of CO$_2$ (∼170° W) with the strongest potential efflux closest to shore (i.e., Nunivak Island; Fig. 7). In these regions, an important caveat is that the presence of sea-ice forms a barrier to air-sea gas exchange. Given that the sea-ice % cover varied between ∼90 % and 100 % and open water area was <10 %, the actual air-sea CO$_2$ flux rates would likely be much smaller (<0–3 mmoles CO$_2$ m^{-2} d^{-1}) similar to other studies of sea-ice covered Arctic Ocean waters (e.g., Bates, 2006; Bates and Mathis, 2009). We recognize however that some studies suggest that sea-ice allows gas exchange (Gosink et al., 1976; Semiletov et al., 2004; Delille et al., 2007; Nagurnyi, 2008; Miller et al., 2011) and so wintertime/springtime air-sea CO$_2$ flux rates may be higher during sea-ice covered conditions.

Over the southern Bering Sea shelf, where sea-ice cover was much less, surface waters between Nunavak Island and the Pribilof Islands had modest influx rates of ∼ −10 to −25 mmoles CO$_2$ m^{-2} d^{-1}. In comparison, our MLR based model climatological maps showed mostly low rates of air-sea CO$_2$ exchange (−10 to +10 mmoles CO$_2$ m^{-2} d^{-1}) across much of the shelf regions, with higher efflux rates occuring in the outershelf (particularly north of St. Matthew Island as in observations), and also offshore (Fig. 6).

3.2.2 Summertime air-sea CO$_2$ fluxes

During the summertime cruise, sea-ice was absent and the Bering Sea shelf had transitioned from mostly neutral conditions to a strong oceanic sink for CO$_2$. In the northern Bering Sea, the rates of air-sea CO$_2$ flux rates varied from −15 to −60 mmoles CO$_2$ m^{-2} d^{-1} (Fig. 7). The exception to this general observation was a small region of CO$_2$ efflux at the innermost shelf station (up to +30 mmoles CO$_2$ m^{-2} d^{-1}). Previous studies have suggested that the nearshore waters were influenced by river runoff (Mathis et al., 2011) which in rivers draining the Arctic landmasses tend to have higher seawater pCO$_2$ values than the atmosphere (e.g., Salisbury et al., 2008). Along the shelf to the west of St. Matthew Island south to the Pribilof Islands in the region of the Bering Sea "*green belt*" and high rates of NCP (Mathis et al., 2010), air-sea CO$_2$ flux rates varied, mostly between −15 and −60 mmoles CO$_2$ m^{-2} d^{-1} with some areas of higher influx (−120 mmoles CO$_2$ m^{-2} d^{-1}) between Nunivak Island and the Pribilof Islands. However, close to the Pribilof Islands, air-sea CO$_2$ flux rates were much reduced (−5 to −25 mmoles CO$_2$ m^{-2} d^{-1}), but a region of CO$_2$ efflux was observed south of the Pribilof Islands (up to +60 mmoles CO$_2$ m^{-2} d^{-1}). In the SE Bering Sea, air-sea CO$_2$ flux rates were close to neutral with no net influx or efflux of CO$_2$. In comparison, our MLR model of climatological air-sea CO$_2$ flux showed that much of the Bering Sea shelf was typically a modest sink for CO$_2$ (with air-sea CO$_2$

flux rates of -10 to -30 mmoles CO$_2$ m^{-2} d^{-1}). In similarity to observational based estimates, there was an air-sea CO$_2$ efflux offshore and at the nearshore stations (Fig. 6).

4 Discussion

4.1 Potential controls on seawater pCO$_2$ and air-sea CO$_2$ gas exchange across the Bering Sea

There are many physical and biological processes that can influence seawater pCO$_2$ and air-sea CO$_2$ gas exchange but the major factors include warming/cooling, the balance of evaporation and precipitation, vertical and horizontal mixing (including entrainment/detrainment; vertical diffusion, and advection), biological uptake/release of CO$_2$ and alkalinity (which are influenced by processes such as surface layer net pelagic phytoplankton primary production, respiration and calcification, export of organic carbon from the surface, sub-surface remineralization, and in a systems framework by the balance of net autotrophy versus heterotrophy; Ducklow and McAllister, 2005), and the process of air-sea gas exchange itself. In nearshore and shallow coastal seas, the contributions of river runoff and sedimentary uptake/release of CO$_2$ and alkalinity (e.g., Thomas et al., 2009) have more importance. In seasonally sea-ice covered waters, sea-ice can act as a barrier to gas exchange (note that there is significant disagreement on this process, Gosink et al., 1976; Semiletov et al., 2004; Delille et al., 2007), carbon export can be facilitated via brine rejection during sea-ice formation (e.g., Omar et al., 2005) and sea-ice melt properties and sea-ice biota can significantly modify surface inorganic carbon properties. Here, we examine the effect of temperature change and ocean biology on seawater pCO$_2$ and air-sea CO$_2$ gas exchange rates on the Bering Sea shelf following a simple empirical analysis similar to methods used to determine the primary controls on temporal and spatial variability of global ocean pCO$_2$ (Takahashi et al., 2002, 2009).

As shown in other studies, the Bering Sea shelf exhibits seasonal spring to summer warming of up to 10 °C. In order to remove the temperature effect from the calculated pCO$_2$, seawater pCO$_2$ values are normalized to a constant temperature of 0 °C using the equation (Takahashi et al., 2002):

$$p\mathrm{CO_2} \text{ at } 0\,°\mathrm{C} = p\mathrm{CO_2}^{\mathrm{obs}} \times \exp[(0.0423(T^{\mathrm{obs}} - 0\,°\mathrm{C}))] \quad (5)$$

where T^{obs} is the observed temperature. This normalization procedure accounts for the thermodynamic effect of warming/cooling on seawater pCO$_2$ which has been experimentally determined at about 4.23 % change in pCO$_2$ per °C change (Takahashi et al., 1993).

Seawater pCO$_2$ temperature normalization can be used to assess the impact of temperature and ocean biology on the seasonal changes in pCO$_2$ observed over the Bering Sea shelf between spring and summer. For regional interpretation, we compute the mean calculated seawater pCO$_2$ difference between spring and summer (δpCO$_2^{\mathrm{spring-summer}}$) and
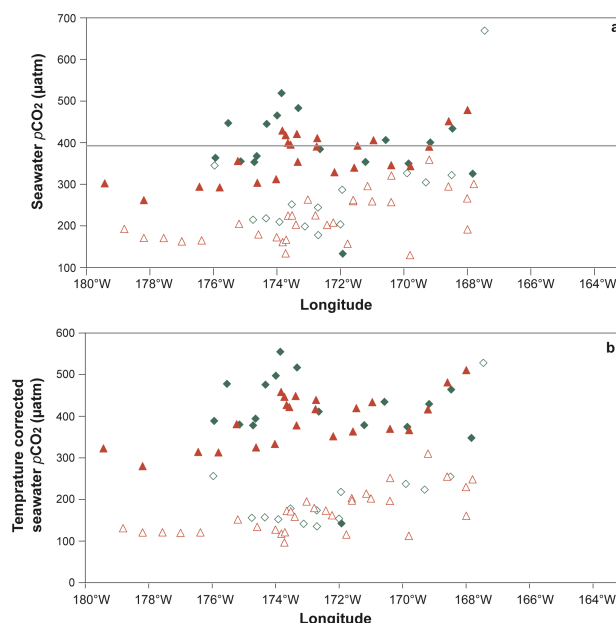

Fig. 8. Surface seawater pCO$_2$ (panel **a**) and temperature corrected seawater pCO$_2$ (panel **b**) plotted against longitude for the northern Bering Sea shelf at the North Line (red symbols) and Middle Line (green symbols). Temperature corrected seawater pCO$_2$ was based on corrected to 0 °C using the empirical relationships of Takahashi et al., 2002. Spring and summer data was shown with closed and open symbols respectively. In the panels, the nearshore to offshore transition is shown from right to left (i.e., east to west).

change in pCO$_2$ due to spring-summer changes in temperature (i.e., δpCO$_2^{\mathrm{temperature}}$ computed using Eq. 6) for five different regions of the Bering Sea shelf, including; (1) the North Line; (2) the Middle Line; (3) between Nunavak Island and Pribilof Islands, (4) south of the Probilof Islands, and; (5) SE Bering Sea shelf. The unknown term, δpCO$_2^{\mathrm{biology}}$, which is the change in seawater pCO$_2$ due to spring-summer changes in ocean biology, is solved from the following equation:

$$\delta p\mathrm{CO_2^{spring-summer}} = \delta p\mathrm{CO_2^{temperature}} + \delta p\mathrm{CO_2^{biology}} \quad (6)$$

This approach follows the empirically based method of Takahashi et al. (2002) in which the term δpCO$_2^{\mathrm{biology}}$, approximates the "net biology" effect or the net balance of photosynthesis and respiration or net community production (NCP).

For the Bering Sea shelf, the "net biology" term largely reflects NCP. However, an important caveat is that the "net biology" term also includes minor contributions from alkalinity changes due to CaCO$_3$ production/dissolution and nitrate utilization, and vertical/horizontal contributions from mixing with subsurface waters or offshore waters, and air-sea CO$_2$ gas exchange. In their estimates of Bering Sea shelf NCP rates, Mathis et al. (2010) calculated that CaCO$_3$ production, and vertical diffusion contributed ~1.5 %, and 2.5–4.5 % to estimates of NCP from DIC changes. Salinity changes as
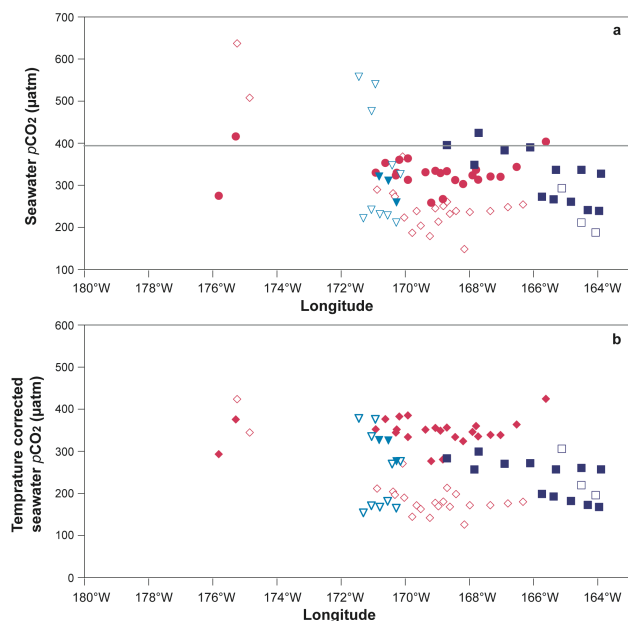
Fig. 9. Surface seawater pCO$_2$ (µatm; panel **a**) and temperature corrected seawater pCO$_2$ (µatm; panel **b**) plotted against longitude for the southern Bering Sea shelf for the following regions: (1) between Nunavak Island and Pribilof Islands (pink symbols); (2) south of Pribilof Islands (blue symbols), and; (3) SE Bering Sea shelf (turquoise symbols). Temperature corrected seawater pCO$_2$ was based on corrected to 0 °C using the empirical relationships of Takahashi et al., 2002. Spring and summer data was shown with closed and open symbols respectively. In the panels, the nearshore to offshore transition is shown from right to left (i.e., east to west).

a result of evaporation and precipitation also have very minor impact on seawater pCO$_2$ since DIC and total alkalinity are changed in equal proportion. Sea-ice melt and river runoff were also considered very minor contributors to the "net biology" term across most of the shelf with only the nearshore areas with salinities lower than 30 showing evidence of minor contributions from river runoff and sea-ice melt (Mathis et al., 2011). In addition, the contribution of advection to the "net biology" term is likely minor given that the water residence time of the outer shelf is 3 months with longer residence times in the middle and inner domains of the Bering Sea shelf (Coachman, 1986). In summary, the inherently simple construct of this approach allows a general view of how seasonal warming or "net biology" (i.e., NCP) influences the CO$_2$ sink or source status of the Bering Sea shelf. As in the Takahashi et al. (2002) approach, we assess whether the effects of seasonal temperature changes on seawater pCO$_2$ exceeds the biological effect (e.g., as in the North Atlantic Ocean subtropical gyre) or the opposite (i.e., "net biology" > temperature; e.g., Ross Sea).
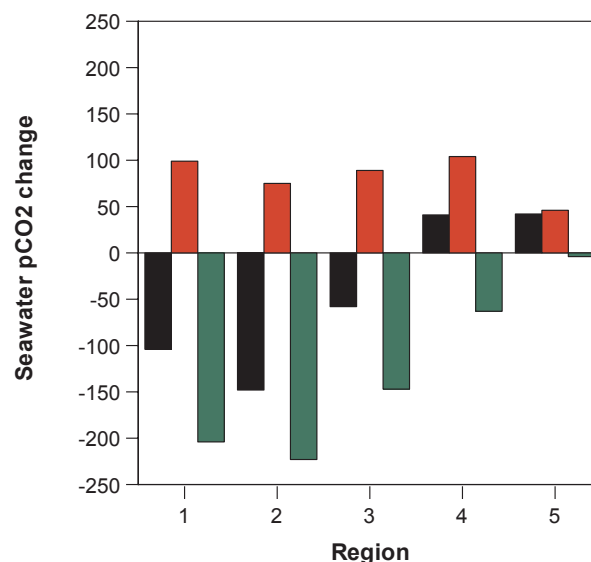

Fig. 10. Temperature and the "net biology" effects on seasonal change in calculated seawater pCO$_2$ (µatm) for the following regions of the Bering Sea shelf: (1) the North Line; (2) the Middle Line; (3) between Nunavak Island and Pribilof Islands, (4) south of the Probilof Islands, and; (5) SE Bering Sea shelf. In the bar chart, the black column denotes the mean observed change in seawater pCO$_2$ for each region (i.e., δpCO$_2^{\text{spring}-\text{summer}}$ in Eq. 7), while the red and green columns indicates the changes imparted by temperature (δpCO$_2^{\text{temperature}}$) and "net biology" (δpCO$_2^{\text{biology}}$), respectively.
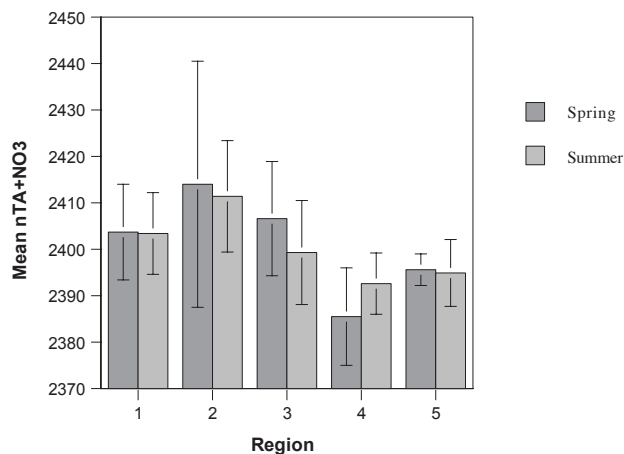

Fig. 11. Spring to summer changes in observed surface nTA+NO$_3$ (µmoles kg^{-1}) for the following regions of the Bering Sea shelf: (1) the North Line; (2) the Middle Line; (3) between Nunavak Island and Pribilof Islands, (4) south of the Probilof Islands, and; (5) SE Bering Sea shelf.

4.1.1 Northern and central Bering Sea shelf

Over the northern and central Bering Sea shelf, there was a seasonal (i.e., spring to summer) drawdown of surface seawater pCO$_2$ of $\sim$100 µatm (Figs. 8 and 9). In the North Line, mean surface seawater pCO$_2$ declined seasonally from 387.5 ± 85.2 µatm to 283.8 ± 123.5 µatm. Similarly in the Middle Line and between Nunivak Island and the Pribilof Islands, mean surface seawater pCO$_2$ declined seasonally from 367.4 ± 56.2 µatm to 219.0 ± 58.0 µatm, and 329.0 ± 35.9 µatm to 270.8 ± 108 µatm, respectively. In comparison to seawater pCO$_2$ changes, temperature corrected seawater pCO$_2$ decreased seasonally by $\sim$200 µatm (Figs. 8 and 9), and up to 300 µatm lower within the "*green belt*" area by the summertime. Thus, in these regions, the "net biology" effect strongly dominated the seasonal change in surface seawater pCO$_2$ compared to warming (Fig. 10). The 2008 BEST data indicates that the "net biology" effect seasonally decreases seawater pCO$_2$ by $\sim$150 to $\sim$230 µatm (Fig. 10) with this drawdown only partially compensated for by an increase in seawater pCO$_2$ due to seasonal warming. For comparison, the Takahashi et al. (2002) climatology suggests that the seasonal drawdown of seawater pCO$_2$ associated with "net biology" effects is $\sim$130–170 µatm. Furthermore, Mathis et al. (2010) show that large seasonal drawdown of DIC results from high rates of NCP particularly within the "*green belt*" area of the Bering Sea shelf. Analysis of seasonal changes in DIC, nitrate and silicate indicated mean Bering Sea shelf NCP rates that ranged from $\sim$20 to 55 mmoles C m^{-2} d^{-1} (Mathis et al., 2010, their Table 4). Within the "*green belt*" area, NCP rates computed from DIC changes ranged from 25 to 47 mmoles C m^{-2} d^{-1} (their Table 3). Given typical mixed layer depth of 30 m and growing season of 80–120 days, the above NCP rates would decrease seawater pCO$_2$ by between $\sim$100 to $\sim$210 µatm similar to our values reported for the "net biology" effect. Our data provides further evidence that "net biology" (which is a near approximate of NCP) dominates the seasonal drawdown of seawater pCO$_2$ for large areas of the Bering Sea shelf. Indeed, seasonal "net biology" effects or spring-summer NCP shifts much of the Bering Sea shelf from a neutral CO$_2$ sink/source status in spring to a strong sink for CO$_2$ by summertime. The vertical export of organic carbon (as a result of high rates of NCP) and it's remineralization back to CO$_2$ in the subsurface appears to result in a buildup of pCO$_2$ in the subsurface (Mathis et al., 2011). Late season mixing and water-column homogenization thus likely restores the Bering Sea shelf to near neutral CO$_2$ sink status in the fall before the wintertime return of sea-ice provides a barrier to further CO$_2$ gas exchange.

4.1.2 Southern Bering Sea shelf

In contrast to the northern and central Bering Sea shelf, warming appears to dominate the seasonal changes of seawater pCO$_2$ for small areas south of the Pribilof Islands

and in the SE Bering Sea shelf region. In these two regions, mean surface seawater pCO$_2$ increased seasonally from 297.1 ± 33.0 µatm to 338.2 ± 137.8 µatm, and from 293.0 ± 55.2 µatm to 324.9 ± 63.2 µatm, respectively. In these two regions, temperature corrected seawater pCO$_2$ decreased seasonally by less than $\sim$50 µatm (Fig. 9). South of the Pribilof Islands, the seasonal "net biology" effect of $\sim$50 µatm was about half of the increase of seawater pCO$_2$ caused by warming (Fig. 10). In these regions, Mathis et al. (2010) compute relatively low rates of NCP of $\sim$12 to 30 mmoles C m^{-2} d^{-1}. In the SE Bering Sea shelf region, there was no seasonal "net biology" effect, and the increase in seawater pCO$_2$ was due to warming only. Surface nitrate data in the SE Bering Sea shelf region were typically below 1 µmoles kg^{-1} for both spring and summer cruises. This suggests that the typical "spring" phytoplankton bloom observed in the SE Bering Sea shelf had occurred earlier than the spring cruise, and that ocean biology had minimal impact on seawater pCO$_2$ and air-sea CO$_2$ fluxes in the spring-summer period. This region also exhibits episodic coccolithophore blooms (e.g., Merico et al., 2004, 2006) that can increase seawater pCO$_2$ (e.g., Bates et al., 1996b; Harley et al., 2010). Previous studies in the SE Bering Sea have shown some evidence for drawdown of alkalinity and increase in seawater pCO$_2$ in late summer of 2000 in response to coccolithophore blooms (Murata and Takizawa, 2002; Murata, 2006). However, there was no evidence in the BEST alkalinity (TA) or calculated seawater pCO$_2$ data for significant impact of coccolithophore blooms in 2008. In all regions, there were no statistically significant changes in salinity normalized TA (i.e., here defined as nTA+NO$_3$ to account for the contribution of nitrate to alkalinity; Brewer and Goldman, 1978) from spring to summer (Fig. 11). nTA+NO$_3$ were slighly lower south of the Pribilof Islands and in the SE Bering Sea shelf compared to other regions which suggests that if coccolithophores contributed significantly to the "spring" phytoplankton bloom, this occurred earlier than the spring cruise. In summary, in contrast to most of the Bering Sea shelf, seasonal warming shifted localized areas of the shelf from minor/neutral CO$_2$ sink status to neutral/minor CO$_2$ source status.

4.2 2008 BEST data in context of seasonal changes in seawater pCO$_2$ and annual air-sea CO$_2$ fluxes

On the Bering Sea shelf, previous studies have shown inorganic carbon data distributions (e.g., Park et al., 1974; Codispoti et al., 1982, 1986; Mathis et al., 2010) but there is very limited data on seawater pCO$_2$ (Kelley and Hood, 1971; Chen, 1993). Several studies report northern Bering Sea shelf seawater pCO$_2$ but these data were collected north of St. Lawrence Island (Murata, 2006; Chen and Gao, 2007) outside the domain of our study. The Takahashi et al. (2009) seawater pCO$_2$ climatology shows a seasonal change of $\sim$50–80 µatm for the Bering Sea shelf with a spring-summer
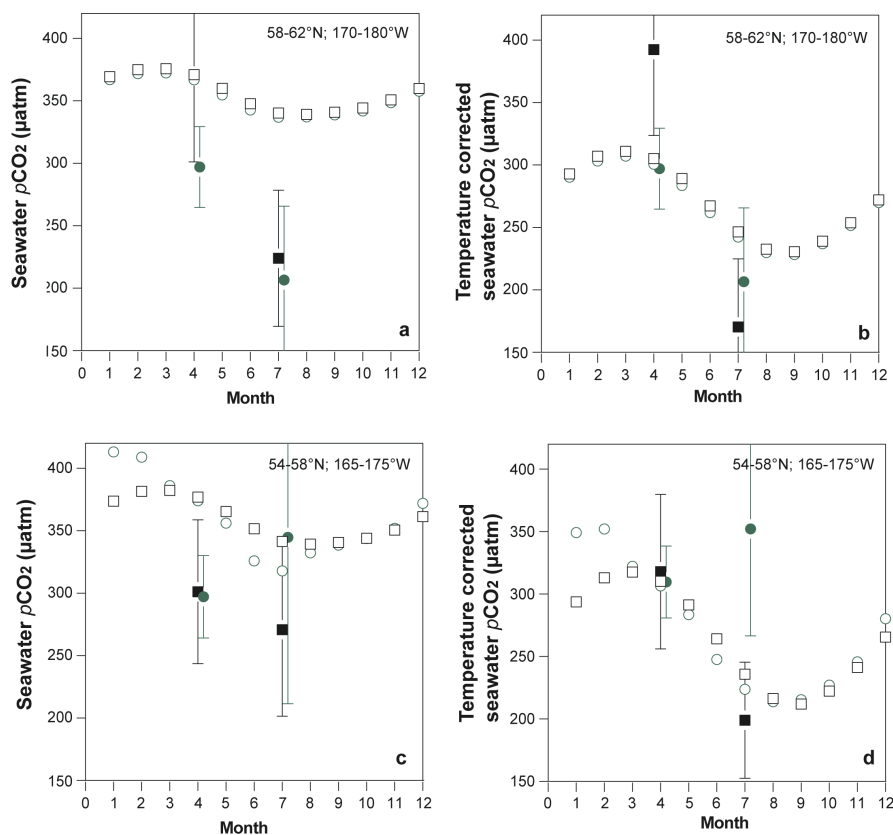
Fig. 12. Comparison of Takahashi et al. (2009) surface seawater pCO_2 and temperature corrected seawater pCO_2 climatology for the Bering Sea shelf with observations from the 2008 BEST spring and summer cruises. The Takahashi et al. (2009) data have a spatial resolution of $4° \times 5°$ and monthly resolution. 2008 BEST spring and summer are binned and averaged within each of four Takahashi et al. (2009) $4° \times 5°$ that are defined for the Bering Sea shelf. Please note that the mean values for observed data from the two $4° \times 5°$ areas have been slightly offset in time to allow for easier interpretation of data. (**a**) surface seawater pCO_2 for the $58°$ N–$62°$ N/$170°$ W–$175°$ W (black symbols), and $58°$ N–$62°$ N/$175°$ W–$180°$ W (green symbols) areas. In each of the panels, Tahahashi et al. (2009) climatology data are shown by open symbols while 2008 BEST spring and summer are shown as closed symbols (mean and 1 std deviation); (**b**) surface temperature corrected seawater pCO_2 for the $58°$ N–$62°$ N/$170°$ W–$175°$ W (black symbols), and $58°$ N–$62°$ N/$175°$ W–$180°$ W (green symbols) areas; (**c**) surface seawater pCO_2 for the $54°$ N–$58°$ N/$165°$ W–$170°$ W (black symbols), and $54°$ N–$58°$ N/$170°$ W–$175°$ W (green symbols) areas; and; (**d**) surface temperature corrected seawater pCO_2 for the $54°$ N–$58°$ N/$165°$ W–$170°$ W (black symbols), and $54°$ N–$58°$ N/$170°$ W–$175°$ W (green symbols) areas. For the temperature corrected seawater pCO_2 datasets, both Takahashi et al. (2009) and 2008 BEST spring and summer data were corrected to 0 °C using the empirical relationships of Takahashi et al. (2002).

drawdown (Fig. 12) that causes the shelf to act as a CO_2 sink ($\sim$1–2 mol C m^{-2} yr^{-1}). However, an important caveat is that the seawater pCO_2 climatology is based on very limited data (1 cruise), and thus it is difficult to draw firm conclusions about the seasonal and annual CO_2 sink-source status of the Bering Sea shelf.

The Takahashi et al. (2009) seawater pCO_2 climatology has four $4° \times 5°$ areas that overlie the Bering Sea shelf (Fig. 12). For July, average ΔpCO_2 values range from -20.8 to -44.7 µatm for these four. In contrast, the 2008 BEST summer mean ΔpCO_2 values ranged from -110.8 µatm to -170.4 µatm for the same areas, indicating that the shelf was much more strongly undersaturated than the seawater pCO_2 climatology suggests. As a consequence, the mean July air-

to-sea CO_2 fluxes calculated here were about 5 times higher ($\sim$ -16.3 to -24.2 mmoles m^{-2} d^{-1}) than the Takahashi et al. (2009) seawater pCO_2 climatology.

Early model studies of Walsh and Dieterle (1994), using data collected by Codispoti et al. (1986), indicated that the annual CO_2 sink was $\sim$4.3 mol C m^{-2} yr^{-1} (Table 1). Based on the air-sea CO_2 flux rate reported by Walsh and Dieterle (1994) and surface area for the Bering Sea shelf, we calculated that the net annual CO_2 sink for the Bering Sea shelf was $\sim$3.4 Tg C yr^{-1} (Table 1). In this and subseqent calculations, we assumed that the surface area of the Bering Sea shelf was $\sim$500 000 km^2, that sea-ice free, open water conditions were typically present for 180 days a year, and that there was not significant gas exchange during sea-ice cover. More

Table 1. Estimates of the annual air-sea CO$_2$ flux on the Bering Sea shelf, assuming 500,000 km^2 of shelf area, and 180 days of open water.

Study	daily flux (mmoles CO$_2$ m^{-2}d^{-1})	annual flux (moles CO$_2$ m^{-2}yr^{-1})	Bering Sea annual flux flux (Tg C yr^{-1})
Walsh and Dieterle (1994)	n/a	4.3	3.4
Chen and Borges	-1.2[a] and 0.66[b]	n/a	11
Tahahashi et al. (2009)	2	n/a	37
This study	22 ± 3	n/a	157 ± 35
Chen et al. (2004)	n/a	n/a	200

[a]Nedashkovskii and Sapozhnikov (2001); [b]Codispoti et al. (1986)

recently, Chen and Borges (2009) summarized coastal air-sea CO$_2$ fluxes, reporting springtime and summertime fluxes of ~ -1.2 mmol C m^{-2} d^{-1} (Nedashkovskii and Sapozhnikov, 2001) and 0.66 mmol C m^{-2} d^{-1} (Codispoti et al., 1986), respectively. If we scale up these flux rates, accounting for Bering Sea surface area and period of open water conditions, we estimate a net annual CO$_2$ sink of ~ 11 Tg C yr^{-1}. Similarly, scaling our observations and the climatology of Takahashi et al. (2009), we compute that the Bering Sea shelf CO$_2$ sink was 157 ± 35 Tg C yr^{-1} and ~ 37 Tg C yr^{-1}, respectively (Table 1). The primary difference between the 2008 BEST datasets and Takahashi et al. (2009) seawater pCO$_2$ climatology relates to the much larger undersaturation observed in surface waters during summertime in 2008 (Fig. 12). Our annual estimate of $157 \pm$ Tg C yr^{-1}, compares to the estimates for the entire Bering Sea of 200 Tg C yr^{-1} previously reported by Chen et al. (2004). In comparison, annual rates of NCP or PP have been estimated at 99 ± 29 Tg C yr^{-1} (Mathis et al., 2010) and 102 Tg C yr^{-1}, respectively (Springer, 1986). Thus the gas exchange term appears to be $\sim 50\%$ higher than the NCP term, at least for 2008.

There are many caveats in scaling any of the above flux data to annual CO$_2$ flux rates and caution must be considered in undertaking this scaling up and interpreting such results. If the 2008 BEST datasets are indeed representative of typical conditions, then the Bering Sea shelf is a much larger CO$_2$ sink than previously thought. At the very least, such uncertainties in providing an accurate assessment of the annual CO$_2$ sink-source status of the Bering Sea shelf, requires future long-term monitoring efforts for this important shelf region. It should also be noted that an extensive coccolithophore bloom was not observed in the Bering Sea in 2008, but this phenomena has been observed in prior years (e.g., Murata and Takizawa, 2002; Murata, 2006; Merico et al., 2004, 2006) and in 2009. Since coccolithophore calcification can result in an increase of seawater pCO$_2$ (e.g., Bates et al., 1996b; Harley et al., 2010), the Bering Sea shelf CO$_2$ sink may be much reduced in those years with significant coccolithophore bloom events, for example, in 2000 (Murata, 2006).

5 Conclusions

Spring observations in 2008 of surface seawater pCO$_2$ ranged from ~ 180 µatm to ~ 520 µatm across the Bering Sea shelf but the presence of sea-ice and relatively small ΔpCO$_2$ gradients suggest that much of the Bering Sea shelf was close to neutral in terms of CO$_2$ sink-source status. Summertime observations of surface seawater pCO$_2$ exhibited a greater range (~ 130 µatm to ~ 640 µatm) than springtime with most of the Bering Sea shelf strongly undersaturated with respect to the atmosphere, and the Bering Sea shelf had transitioned from mostly neutral conditions to a stronger oceanic sink for atmospheric CO$_2$. Our data further suggests that biological processes (as evidenced by high rates of NCP for the shelf; Mathis et al., 2010) dominates the seasonal drawdown of seawater pCO$_2$ for large areas of the Bering Sea shelf during late spring and summer, with the effect partly countered by seasonal warming, particularly in the southeastern Bering Sea. Thus seasonal "net biology" effects strongly shift much of the Bering Sea shelf from a neutral CO$_2$ sink/source status in spring to a strong oceanic sink for CO$_2$ by summertime. Although our data does not include fall or winter data, we anticipate that late season mixing restores the Bering Sea shelf to near neutral CO$_2$ sink status before sea-ice provides a barrier to further CO$_2$ gas exchange. In small areas of the Bering Sea shelf south of the Pribilof Islands and in the SE Bering Sea, seasonal warming is the dominant influence on seawater pCO$_2$, shifting localized areas of the shelf from minor/neutral CO$_2$ sink status to neutral/minor CO$_2$ source status, in contrast to much of the surrounding Bering Sea shelf. Overall, the Bering Sea shelf appears to be a stronger sink for atmospheric CO$_2$ than previously suggested by the Takahashi et al. (2009) seawater pCO$_2$ climatology. Given that Bering Sea shelf is the largest US coastal shelf sea, we suggest that future long-term monitoring of the region is critical for assessments of the contribution of the Bering Sea shelf to regional carbon budgets and evaluation of seasonal and interannual variability in response to natural and anthropogenically influenced climate change.

References

Antonov, J. I., Locarnini, R. A., Boyer, T. P., Mishonov, A. V., and Garcia, H. E.: World Ocean Atlas 2005, Volume 2: Salinity, edited by: Levitus, S., NOAA Atlas NESDIS 62, US Government Printing Office, Washington, DC, 182 pp., 2006.

Banse, K. and English, D. C.: Comparing phytoplankton seasonality in the Eastern and Western subarctic Pacific and the Western Bering Sea, Prog. Oceanogr., 43, 235–288, 1999.

Bates, N. R.: Air-sea CO_2 fluxes and the continental shelf pump of carbon in the Chukchi Sea adjacent to the Arctic Ocean, J. Geophys. Res.-Oceans, 111, C10013, doi:10.129/2005JC003083, 12 October 2006.

Bates, N. R. and Mathis, J. T.: The Arctic Ocean marine carbon cycle: evaluation of air-sea CO_2 exchanges, ocean acidification impacts and potential feedbacks, Biogeosciences, 6, 2433–2459, doi:10.5194/bg-6-2433-2009, 2009.

Bates, N. R., Michaels, A. F., and Knap, A. H.: Seasonal and interannual variability of the oceanic carbon dioxide system at the US JGOFS Bermuda Atlantic Time-series Site, Deep-Sea Res. Pt. II, 43(2–3), 347–383, doi:10.1016/0967-0645(95)00093-3, 1996a.

Bates, N. R., Michaels, A. F., and Knap, A. H.: Alkalinity changes in the Sargasso Sea: Geochemical evidence of calcification?, Mar. Chem., 51(4), 347–358, doi:10.1016/0304-4203(95)00068-2, 1996b.

Bates, N. R., Pequignet, A. C., and Sabine, C. L.: Ocean carbon cycling in the Indian Ocean: II. Estimates of net community production, Global Biogeochem. Cy., 20(3), GB3021, doi:10.1029/2005GB002492, 2006b.

Bates, N. R., Pequignet, A. C., and Sabine, C. L.: Ocean carbon cycling in the Indian Ocean: 1. Spatiotemporal variability of inorganic carbon and air-sea CO_2 gas exchange, Global Biogeochem. Cy., 20(3), GB3020, doi:10.1029/2005GB002491, 2006a.

Bond, N. A., Overland, J. E., Spillane, M., and Stabeno, P.: Recent shifts in the state of the North Pacific, Geophys. Res. Lett., 30(23), 2183, doi:10.1029/2003GL018597, 2003.

Bond, N. A. and Overland, J. E.: The importance of episodic weather events to the ecosystem of the Bering Sea shelf, Fish. Oceanogr., 14(2), 97–111, 2005.

Brewer, P. G. and Goldman, J. C.: Alkalinity changes generated by phytoplankton growth, Limnol. Oceanogr., 21(1), 108–117, 1976.

Broerse, A. T. C., Tyrell, T., Young, J. R., Poulton, A. J., Merico, A., Balch, W. M., and Miller, P. I.: The cause of bright waters in the Bering Sea in winter, Cont. Shelf Res., 23, 1579–1596, 2003.

Chen, C. T.-A.: Carbonate chemisrty of the wintertime Bering Sea marginal ice zone, Cont. Shelf Res., 13(1), 67–87, 1993.

Chen, C. T. A. and Borges, A. V.: Reconciling opposing views on carbon cycling in the coastal ocean: continental shelves as sinks and near-shore ecosystems as sources of atmospheric CO_2, Deep-Sea Res. Pt. II, 56(8–10), 578–581, doi:10.1016/j.dsr2.2009.01.001, 2009.

Chen, C. T.-A., Andreev, A., Kim, K. R., and Yamamoto, M.: Roles of continental shelves and marginal seas in the biogeochemical cycles of the North Pacific Ocean, J. Oceanogr., 60(1), 17–44, 2004.

Chen, L. and Gao, Z.: Spatial variability in the partial pressures of CO_2 in the Northern Bering and Chukchi seas, Deep-Sea Res. Pt. II, 54, 2619–2629, 2007.

Coachman, L. K.: Circulation, water masses, and fluxes on the southeastern Bering Sea shelf, Cont. Shelf Res., 5, 23–108, 1986.

Coatanoan, C., Goyet, C., Gruber, N., Sabine, C. L., and Warner, M.: Comparison of two approaches to quantify anthropogenic CO_2 in the ocean: results from the northern Indian Ocean, Global Biogeochem. Cy., 15, 11–25, 2001.

Codispoti, L. A., Friederich, G. E., Iverson, R. L., and Hood, D. W.: Temporal changes in the inorganic carbon system of the Southeastern Bering Sea during spring 1980, Nature, 296, 242–245, 1982.

Codispoti, L. A., Friederich, G. E., and Hood, D. W.: Variability in the inorganic carbon system over the Southeastern Bering Sea shelf during spring 1980 and spring-summer 1981, Cont. Shelf Res., 5, 133–160, 1986.

Comiso, J. C., Parkinson, C. L., Gersten, R., and Stock, L.: Accelerated decline in the Arctic sea ice cover, Geophys. Res. Lett., 35, L01703, doi:10.1029/2007GL031972, 2008.

Delille, B., Jourdain, B., Borges, A. V., Tison, J.-L., and Delille, D.: Biogas (CO_2, O_2, dimethylsulfide) dynamics in spring Antarctic fast ice, Limnol. Oceanogr., 52, 1367–1379, 2007.

Dickson, A. G. and Millero, F. J.: A comparison of the equilibrium constants for the dissociation of carbonic acid in seawater media, Deep-Sea Res., 34, 1733–1743, 1987.

Dickson, A. G., Sabine, C. L., and Christian, J. R.: Guide to best practices for ocean CO_2 measurements, Sidney, British Columbia, North Pacific Marine Science Organization, PICES Special Publication 3, 2007.

Ducklow, H. W. and McAllister, S. L.: Biogeochemistry of carbon dioxide in the coastal oceans, in: The Sea, Volume 13, The Global Coastal Ocean-Multiscale Interdisciplinary Processes, edited by: Robinson, A. R. and Brink, K., J. Wiley and Sons, NY, 2005.

Garcia, H. E., Locarnini, R. A., Boyer, T. P., and Antonov, J. I.: World Ocean Atlas 2005, Volume 3: Dissolved Oxygen, Apparent Oxygen Utilization, and Oxygen Saturation, edited by: Levitus, S., NOAA Atlas NESDIS 63, US Government Printing Office, Washington, DC, 342 pp., 2006a.

Garcia, H. E., Locarnini, R. A., Boyer, T. P., and Antonov, J. I.: World Ocean Atlas 2005, Volume 4: Nutrients (phosphate, nitrate, silicate), edited by: Levitus, S., NOAA Atlas NESDIS 64, US Government Printing Office, Washington, DC, 396 pp., 2006b.

GLOBALVIEW-CO_2: Cooperative Atmospheric Data Integration Project for Carbon Dioxide, 2007, CD-ROM, NOAA CMDL, Boulder, CO, also available on Internet via anonymous FTP to

ftp.cmdl.noaa.gov, Path: ccg/co2/GLOBALVIEW, 2007.

Gosink, T. A., Pearson, J. G., and Kelley, J. J.: Gas movement through sea ice, Nature, 263, 41–42, doi:10.1038/263041al, 1976.

Goyet, C. and Poisson, A. P.: New determination of carbonic acid dissociation constants in seawater as a function of temperature and salinity, Deep-Sea Res., 36, 1635–1654, 1989.

Goyet, C. and Davis, D.: Estimation of total CO$_2$ concentration throughout the water column, Limnol. Oceanogr., 44, 859–877, 1997.

Grebmeier, J. M., Cooper, L. W., Feder, H. M., and Sirenko, B. I.: Ecosystem dynamics of the Pacific-influenced Northern Bering and Chukchi Seas in the Amerasian Arctic, Prog. Oceanogr., 71(2–4), 331–361, 2006a.

Grebmeier, J. M., Overland, J. E., Moore, S. E., Farley, E. V., Carmack, E. C., Cooper, L. W., Frey, K. E., Helle, J. H., McLaughlin, F. A., and McNutt, S. L.: A major ecosystem shift in the Northern Bering Sea, Science, 311(5766), 1461–1464, 2006b.

Grebmeier, J. M., Bates, N. R., and Devol, A.: Continental Margins of the Arctic Ocean and Bering Sea, in: North American Continental Margins: A Synthesis and Planning Workshop, edited by: Hales, B., Cai, W.-J., Mitchell, B. G., Sabine, C. L., and Schofield, O., 120 pp., 61–72, 2008.

Hansell, D. A., Goering, J. J., Walsh, J. J., McRoy, C. P., Coachman, L. K., and Whitledge, T. E.: Summer phytoplankton production and transport along the shelf break front in the Bering Sea, Cont. Shelf Res., 9, 1085–1104, 1989.

Harley, J., Borges, A. V., Van Der Zee, C., Delille, B., Godi, R. H. M., Schiettecatte, L.-S., Roevros, N., Aerts, K., Plapernat, P.-E., Rebreanu, L., Groom, S., Daro, M.-H., Van Grieken, R., and Chou, L.: Biogeochemical study of coccolithophore bloom in the northern Bay of Biscay (NE Atlantic Ocean) in June 2004, Prog. Oceeanogr., 86, 317–336, doi:10.1016/j.pocean.23010.04.029, 2010.

Hollowed, A. B., Hare, S. R., and Wooster, W. S.: Pacific Basin climate variability and patterns of Northeast Pacific marine fish populations, Prog. Oceanogr., 49, 257–282, 2001.

Hunt, G. L., Stabeno, P., Walters, G., Sinclair, E., Brodeur, R. D., Napp, J. M., and Bond, N. A.: Climate change and control of the Southeastern Bering Sea pelagic ecosystem, Deep-Sea Res. Pt. II, 49(26), 5821–5853, 2002.

Kelley, J. J. and Hood, D. W.: Carbon dioxide in the surface water of the ice-covered Bering Sea, Nature, 229, 37–39, 1971.

Key, R. M., Kozyr, A., Sabine, C. L., Lee, K., Wanninkhof, R., Bullister, J. L., Feely, R. A., Millero, F. J., Mordy, C., and Peng, T.-H.: A global ocean carbon climatology: results from Global Data Analysis Project (GLODAP), Global Biogeochem. Cy., 18, GB4031, doi:10.1029/2004GB002247, 2004.

Lee, K.: Global net community production estimated from the annual cycle of surface water total dissolved inorganic carbon, Limnol. Oceanogr., 46(6), 1287–1297, 2001.

Lee, K., Karl, D. M., Wanninkhof, R., and Zhang, J. Z.: Global estimates of net carbon production in the nitrate-depleted tropical and subtropical oceans, Geophys. Res. Lett., 29(19), 1907, 2002.

Locarnini, R. A., Mishonov, A. V., Antonov, J. I., Boyer, T. P., and Garcia, H. E.: World Ocean Atlas 2005, Volume 1: Temperature, edited by: Levitus, S., NOAA Atlas NESDIS 61, US Government Printing Office, Washington, DC, 182 pp., 2006.

Macklin, S. A., Hunt, G. L., and Overland, J. E.: Collaborative re-

search on the pelagic ecosystem of the Southeastern Bering Sea shelf, Deep-Sea Res. Pt. II, 49(26), 5813–5819, 2002.

Mathis, J. T., Cross, J. N., Bates, N. R., Bradley Moran, S., Lomas, M. W., Mordy, C. W., and Stabeno, P. J.: Seasonal distribution of dissolved inorganic carbon and net community production on the Bering Sea shelf, Biogeosciences, 7, 1769–1787, doi:10.5194/bg-7-1769-2010, 2010.

Mathis, J. T., Cross, J., and Bates, N. R.: Coupling primary production and terrestrial runoff to ocean acidification and carbonate mineral suppression in the eastern Bering Sea, Global Biogeochem. Cy., 116, C02030, doi:10.1029/2010JC006453, 2011.

McRoy, C. P. and Goering, J. J.: The influence of ice on the primary productivity of the Bering Sea, in: Oceanography of the Bering Sea with Emphasis on Renewable Resources, edited by: Hood, D. W. and Kelley, E. J., Univ. of Alaska, Fairbanks, 403–421, 1974.

Mehrbach, C., Culberson, C. H., Hawley, J. E., and Pytkowicz, R. M.: Measurement of the apparent dissociation constants of carbonic acid in seawater at atmospheric pressure, Limnol. Oceanogr., 18, 897–907, 1973.

Merico, A., Tyrrell, T., Lessard, E. J., Oguz, T., Stabeno, P. J., Zeeman, S. I., and Whitledge, T. E.: Modelling phytoplankton succession on the Bering Sea role of climate influences and trophic interactions in generating *Emiliania huxleyi* blooms 1997–2000, Deep-Sea Res. Pt. I, 51(12), 1803–1826, 2004.

Merico, A., Tyrrell, T., and Cokacar, T.: Is there any relationship between phytoplankton seasonal dynamics and the carbonate system? J. Marine Syst., 59(1–2), 120–142, 2006.

Midorikawa, T., Umeda, T., Hiraishi, N., Ogawa, K., Nemoto, K., Kubo, N., and Ishii, M.: Estimation of seasonal net community production and air-sea CO$_2$ flux based on the carbon budget above the temperature minimum layer in the Western subarctic North Pacific, Deep-Sea Res. Pt. I, 49(2), 339–362, 2002.

Miller, L. A., Papakyriakou, T. N., Collins, R. E., Deming, J. W., Ehn, J., Macdonald, R. W., Mucci, A., Owens, O., Raudsepp, M., and Sutherland, N.: Carbon dynamics in Sea Ice: A Winter Flux Time Series, J. Geophys. Res., 116, C02028, doi:0.1029/2009JC006058, 2011.

Millero, F. J., Graham, T. B., Huang, F., Bustos-Serrano, H., and Pierrot, D.: Dissociation constants of carbonic acid in seawater as a function of salinity and temperature, Mar. Chem., 100, 80–94, 2006.

Murata, A. and Takizawa, T.: Impact of a coccolithophorid bloom on the CO$_2$ system in surface waters of the Eastern Bering Sea shelf, Geophys. Res. Lett., 29(11), 1547, 2002.

Murata, A.: Increased surface seawater pCO$_2$ in the eastern Bering Sea shelf: an effect of blooms of coccolithophorid Emiliania huxleyi?, Global Biogeochem. Cy., GB4006, doi:10.1029/2005GB002615, 2006.

Murphy, P. P., Nojiri, Y., Harrison, D. E., and Larkin, N. K.: Scales of spatial variability for surface ocean pCO$_2$ in the Gulf of Alaska and Bering Sea: toward a sampling strategy, Geophys. Res. Lett., 28(6), 1047–1050, 2001.

Nagurnyi, A. P.: On the role of Arctic sea-ice in seasonal variability of carbon dioxide concentration in Northern Latitudes, Russ. Meteor. Hydrol., 33(1), 43–47, 2008.

Napp, J. M. and Hunt, G. L.: Anomalous conditions in the South-Eastern Bering Sea 1997: linkages among climate, weather, ocean, and biology, Fish. Oceanogr., 10, 61–68, 2001.

Nedashkovskii, A. P. and Sapozhnikov, V. V.: Estimation of the CO$_2$ fluxes through the ocean-atmosphere boundary by hydrochemical parameters in the western part of the Bering Sea, Oceanology, 41(3), 351–359, 2001.

Okkonen, S. R., Schmidt, G. M., Cokelet, E. D., and Stabeno, P. J.: Satellite and hydrographic observations of the Bering Sea "Green Belt", Deep-Sea Res. Pt. II, 51(10–11), 1033–1051, 2004.

Omar, A., Johannessen, T., Bellerby, R. G. J., Olsen, A., Anderson, L. G., and Kivimäe, C.: Sea ice and brine formation in Storfjorden: implications for the Arctic wintertime air-sea CO$_2$ flux, in: The Nordic Seas: An Integrated Perspective: Oceanography, Climatology, Biogeochemistry, and Modeling, edited by: Drange, H., Dokken, T., Furevik, T., Gerdes, R., and Berger, W., Geoph. Monog., 158, 177–187, 2005.

Park, P. K., Gordon, L. I., and Alvarez-Borego, S.: The carbon dioxide system of the Bering Sea, in: Oceanography of the Bering Sea, edited by: Hood, D. W. and Kelley, J. J., Fairbanks, AK, Institute of marine Sciences, University of Alaska, 107–147, 1974.

Piepenburg, D.: Recent research on Arctic benthos: common notions need to be revised, Polar Biol., 28(10), 733–755, 2005.

Rho, T. and Whitledge, T. E.: Characteristics of seasonal and spatial variations of primary production over the Southeastern Bering Sea shelf, Cont. Shelf Res., 27(20), 2556–2569, 2007.

Ridgwell, A., Zondervan, I., Hargreaves, J. C., Bijma, J., and Lenton, T. M.: Assessing the potential long-term increase of oceanic fossil fuel CO$_2$ uptake due to CO$_2$-calcification feedback, Biogeosciences, 4, 481–492, doi:10.5194/bg-4-481-2007, 2007.

Riebesell, U., Zondervan, I., Rost, B., Tortell, P. D., Zeebe, R. E., and Morel, F. M. M.: Reduced calcification of marine plankton in response to increased atmospheric CO$_2$, Nature, 407, 364–367, 2000.

Robbins, L. L., Hansen, M. E., Kleypas, J. A., and Meylan, S. C.: CO2calc: a user-friendly seawater carbon calculator for Windows, Max OS X, and iOS (iPhone). U.S. Geological Survey Open-File Report, 2010–1280, 1–17, http://pubs.usgs.gov/of/2010/1280/, 2010.

Robertson, J. E., Turner, D. R., Holligan, P. M., Watson, A. J., Boyd, P., Fernandez, E., and Finch, M.: The impact of a coccolithophore bloom on oceanic carbon uptake in the northeast Atlantic during summer 1991, Deep-Sea Res., 41, 297–314, 1994.

Roy, R. N., Roy, L. N., Vogel, R., Moore, C. P., Pearson, T., Good, C. E., Millero, F. J., and Campbell, D.: Determination of the ionization constants of carbonic acid in seawater, Mar. Chem., 44, 249–268, 1993.

Sabine, C. L., Key, R. M., Johnson, K. M., Millero, F. J., Poisson, A. P., Sarmiento, J. L., Wallace, D. W. R., and Winn, C. D.: Anthropogenic CO$_2$ inventory of the Indian Ocean, Global Biogeochem. Cy., 13, 179–198, 1999.

Sabine, C. L. and Feely, R. A.: Comparison of recent Indian Ocean anthropogenic CO$_2$ estimates with a historical approach, Global Biogeochem. Cy., 15, 31–42, 2001.

Salisbury, J. E., Green, M., Hunt, C., and Campbell, J.: Coastal acidification by rivers: A threat to shellfish? EOS, American Geophysical Union Transactions, 89(50), 513–528, 2008.

Semiletov, I., Makshatas, A. I., Akasofu, S.-I. and Andreas, E. L.: Atmospheric CO$_2$ balance: The role of arctic sea ice, Geophys. Res. Lett., 31(5), L05121, doi:10.1029/2003GL017996, 2004.

Serreze, M. C., Holland, M. M., and Stroeve, J.: Perspectives on the Arctic's shrinking sea-ice cover, Science, 315(5818), 1533–1536, doi:10.1126/science.1139426, 2007.

Springer, A. M., McRoy, C. P., and Flint, M. V.: The Bering Sea Green Belt: shelf-edge processes and ecosystem production, Fish. Oceanogr., 5, 205–223, 1996.

Stabeno, P. J., Bond, N. A., Kachel, N. B., Salo, S. A., and Schumacher, J. D.: On the temporal variability of the physical environment over the Southeastern Bering Sea, Fish. Oceanogr., 10, 81–98, 2001.

Stabeno, P. J., Kachel, N. B., Sullivan, M., Whitledge, T. E.: Variability of physical and chemical characteristics along the 70-m isobath of the Southeastern Bering Sea, Deep-Sea Res. Pt. II, 49, 5931–5943, 2002.

Stockwell, D. A., Whitledge, T. E., Zeeman, S. I., Coyle, K. O., Napp, J. M., Brodeur, R. D., Pinchuk, A. I., and Hunt, G. L.: Anomalous conditions in the South-Eastern Bering Sea, 1997: nutrients, phytoplankton and zooplankton, Fish. Oceanogr. 10, 99–116, 2001.

Takahashi, T., Olafsson, J., Goddard, J. G., Chipman, D. W., and Sutherland, S. G.: Seasonal variation of CO$_2$ and nutrients in the high-latitude surface oceans: a comparative study, Global Biogeochem. Cy., 7(4), 843–878, 1993.

Takahashi, T., Sutherland, S. G., Sweeney, C., Poisson, A. P., Metzl, N., Tilbrook, B., Bates, N. R., Wanninkhof, R. H., Feely, R. A., Sabine, C. L., and Olafsson, J.: Biological and temperature effects on seasonal changes of pCO$_2$ in global ocean surface waters, Deep-Sea Res. Pt. II, 49, 1601–1622, 2002.

Takahashi, T., Sutherland, S. C., Wanninkhof, R., Sweeney, C., Feely, R. A., Chipman, D. W., Hales, B., Friederich, G. E., Chavez, F. P., Watson, A. J., Bakker, D. C. E., Schuster, U., Metzl, N., Yoshikawa-Inoue, H., Olafsson, J., Arnarson, T. S., Tilbrook, B., Johannessen, T., Olsen, A., Bellerby, R. J., Nojiri, Y., Wong, C. S., Delille, B., Bates, N. R., and de Baar, H. J. W.: Climatological mean and decadal change in surface ocean pCO$_2$, and net sea-air CO$_2$ flux over the global oceans, Deep-Sea Res. Pt. II, 56, 554–577, 2009.

Thomas, H., Schiettecatte, L.-S., Suykens, K., Koné, Y. J. M., Shadwick, E. H., Prowe, A. E. F., Bozec, Y., de Baar, H. J. W., and Borges, A. V.: Enhanced ocean carbon storage from anaerobic alkalinity generation in coastal sediments, Biogeosciences, 6, 267–274, doi:10.5194/bg-6-267-2009, 2009.

Walsh, J. J. and Dieterle, D. A.: CO$_2$ cycling in the coastal ocean. I – A numerical analysis of the Southeastern Bering Sea with applications to the Chukchi Sea and the Northern Gulf of Mexico, Progr. Oceanogr., 74, 335–392, 1994.

Walsh, J. J., Dieterle, D. A., Muller-Karger, F. E., Aagaard, K., Roach, A. T., Whitledge, T. E., and Stockwell, D.: CO$_2$ cycling in the coastal ocean. II. Seasonal organic loading of the Arctic Ocean from sources waters in the Bering Sea, Cont. Shelf Res., 17(1), 1–36, 1996.

Wanninkhof, R.: Relationship between wind speed and gas exchange over the ocean, J. Geophys. Res., 97, 7373–7382, 1992.

Weiss, R. F.: Carbon dioxide in water and seawater: the solubility of a non-ideal gas, Mar. Chem., 2, 203–215, 1974.

Wong, C. S., Waser, N. A. D., Nojiri, Y., Whitney, F. A., Page J. S., and Zeng, J.: Seasonal and interannual variability in the distribution of surface nutrients and dissolved inorganic carbon in the Northern North Pacific: influence of El Nino, J. Oceanogr., 58(2), 227–243, 2002.

Wyllie-Echeverria, T. and Ohtani, K.: Seasonal sea ice variability and the Bering Sea ecosystem, in: Dynamics of the Bering Sea, edited by: Loughlin, T. and Ohtani, K., Univ. of Alaska Sea Grant Press, Fairbanks, Alaska, 435–451, 1999.

Zeebe, R. and Wolf-Gladrow, D.: CO$_2$ in Seawater: Equilibrium, Kinetics, Isotopes, Elsevier Oceanography Series 65, 2001.

Zondervan, I., Zeebe, R. E., Rost, B, and Riebesell, U.: Decreasing marine biogenic calcification: a negative feedback on rising atmospheric pCO$_2$, Global Biogeochem. Cy., 15, 507–516, 2001.